European Journal of Pharmaceutics and Biopharmaceutics 71 (2009) 318–324

Contents lists available at ScienceDirect

European Journal of Pharmaceutics and Biopharmaceutics

journal homepage: www.elsevier.com/locate/ejpb

Research paper

The permeability of large molecular weight solutes following particle delivery to air-interfaced cells that model the respiratory mucosa

C.I. Grainger [a], L.L. Greenwell [b], G.P. Martin [a], B. Forbes [a,*]

[a] King's College London, Pharmaceutical Science Division, London, UK
[b] Safety and Environmental Assurance Centre, Unilever Colworth, Stambrook, Bedfordshire, UK

ARTICLE INFO

Article history:
Received 23 June 2008
Accepted in revised form 13 September 2008
Available online 25 September 2008

Keywords:
Twin-stage impinger
Calu-3
Deposition
Particle

ABSTRACT

The transepithelial transport rates of compounds after deposition as aerosolised particles onto respiratory cell layers and allowing dissolution in the cell surface secretions has not been reported in a comprehensive manner to date. Here, the twin-stage impinger (TSI) was used to deposit potentially respirable particles (aerodynamically <6.4 μm) of varying molecular weight dextrans labelled with fluorescein isothiocyanate (FITC-dex) onto Calu-3 cells, a model of the bronchial epithelium. The TSI functioned as a particle size segregator, with >96% of the deposited particles being geometrically <6.4 μm (as measured by microscopy) and the particles being deposited discretely with a uniform distribution. Cell layers tolerated particle deposition at an air flow of 60 L/min. A small reduction in transepithelial electrical resistance (TER) of <10% occurred initially, but the original TER was recovered within 10 min and there was no significant effect on apparent permeability (P_{app}) of FITC-dex 4 over 4 h. Interleukin 8 (IL-8) secretion in the apical and basolateral directions over 24 h was not increased by exposure to the TSI and particle deposition. The rate of FITC-dex 4 (4 kDa) transport across the cell layer after deposition and dissolution of the particles in the cell surface secretions was ~20-fold higher ($P < 0.05$) than if applied as a solution. The volume of cell surface secretions was estimated by tracer dilution (3.44 ± 1.90 μl, mean ± SEM) and this value was used to calculate the P_{app} of compound once deposited as a particle. The Papp value was found to be similar to that obtained when the compound was applied in solution ($P < 0.05$). Thus, the increased transport rate was attributable to the differences in donor chamber solute concentration rather than any change in the permeability of the cell layer itself. Following particle deposition, transport of FITC-dex with molecular weights between 4 and 70 kDa correlated well ($r^2 = 0.918$) with reported *in vivo* canine pulmonary clearance after intratracheal instillation of dextrans of similar molecular weight. The use of the TSI and the Calu-3 cell line for the assessment of compound dissolution and transport rates after particle deposition may allow more realistic analyses to be made with respect to the *in vivo* situation.

1. Introduction

Most *in vitro* investigations of respiratory epithelial permeability or toxicity involve the application of test materials to layers of pulmonary epithelial cells as solutions or suspensions [1–9]. Within the lung, however, compounds are presented to the epithelial lining fluid as aerosolised solid particles or liquid droplets. Unless cleared by the mucociliary transport system or macrophages (bioresistant particles), particles deposited on the mucosal surface undergo dissolution followed by solute transport across the epithelium (biodegradable particles). Thus the process of particle dissolution *in vivo* presents a significantly different situation from the application of a solution to respiratory epithelial cells. Some of the major differences in presenting a compound to a cell layer as a particle as opposed to a solution are summarised in Table 1.

Compounds in solution present a uniform concentration over the surface of the cell layer. However, in the case of compounds administered as an aerosol, dissolution into the cell layer lining fluid (or spreading in the case of a deposited liquid droplet) can be envisaged to produce a concentration gradient. A saturated system may be produced immediately adjacent to the particle, with a decreasing concentration as a function of distance from the particle, which is dependent on the dynamics of lateral diffusion in the cell layer lining fluid and partition into the cell layer itself. Non-uniform exposure across the surface of the cell layer may be expected to affect toxicity and absorption profiles, but to date, there have been few attempts to evaluate this *in vitro*.

Although bespoke apparatuses have been developed to apply particles to cell-layers, they are highly technical and costly to setup [10,11]. The most relevant studies to date have been performed using adaptations of relatively simple and commercially available

* Corresponding author. King's College London, Pharmaceutical Science Division, 150 Stamford Street, London SE1 9NH, UK. Tel.: +44 130640515.
E-mail address: Ben.Forbes@kcl.ac.uk (B. Forbes).

0939-6411/$ - see front matter © 2009 Published by Elsevier B.V.
doi:10.1016/j.ejpb.2008.09.006

Table 1
A comparison between the use of cell systems to model solute permeability or toxicity to the respiratory epithelium of compounds following application as a solution compared to application as a particle

	Application as a solution	Deposition of particles
Application of test materials	Layering of a solution upon the mucosal surface of the epithelial cells	Impaction of aerosol particles onto the mucosal surface of the epithelial cells
Mucosal lining fluid volume	Cells submerged under the applied solution	Cells remain at an air-interfaced condition
Mucosal lining fluid composition	Minimal effects of cell secretions on volume or composition of the applied medium	Glycoprotein rich (mucus) or surfactant rich (alveolar) fluid which is the product of cell secretions
Effect of test material	Uniform concentration across the epithelial surface. No influence of particle properties	Concentrations across the epithelial surface range from saturated to low concentrations. Solid state properties influence dissolution

apparatuses such as the twin-stage impinger (TSI), Andersen cascade impactor (ACI) and multi-stage liquid impinger (MSLI) [12–14]. For example, the MSLI has been used to deposit porous microparticles impregnated with sodium fluorescein (flu–Na) onto Calu-3 cell layers [12]. Once deposited, particles were immediately solubilised by the addition of a fluid to allow transepithelial electrical resistance (TER) to be measured and a starting concentration to be known. However, because of the addition of fluid immediately after particle deposition, particles did not dissolve within the cell surface fluid and the dissolution-transfer process that occurs *in vivo* was not modelled.

In this study, the TSI was adapted to accommodate a Calu-3 cell layer (an air-interface cell culture model of the bronchial epithelium which secretes a glycoprotein rich mucus layer [15]) in the lower chamber where respirable particles of an aerodynamic diameter <6.4 μm were deposited. This system allowed deposition of aerosols onto the surface of air-interfaced cell layers, producing a more representative exposure scenario for the assessment of mucosa-particle interaction in terms of toxicology and dissolution limiting permeability to that occurring *in vivo*. The objective of this work was to determine the extent to which the administration of compounds in particulate form would reproduce the transport kinetics observed *in vivo* and to evaluate these in relation to the permeability of the same compounds applied as aqueous solutions.

2. Materials

All materials were obtained from Sigma–Aldrich (Dorset, UK) unless otherwise stated. Cell culture flasks (75 cm^2 with ventilated caps) and Transwell cell culture systems (0.33 cm^2 polyester, 0.4 μm pore size) were from Costar (through Fisher Scientific, Leicestershire, UK). Cell culture reagents included trypsin/ethylene diamine tetraacetate sodium (EDTA) solution (2.5 g/L trypsin, 0.5 g/L EDTA), Hank's balanced salt solution [HBSS, no phenol red, including NaHCO3 at 0.33 g/L with HEPES buffer (0.01 M)], phosphate buffered saline (PBS; Oxoid, Hampshire, UK) and Dulbecco's modified Eagle's/F-12 Ham's (1:1). Black 96-well plates were from Nunc (through Fisher Scientific, Leicestershire, UK). High binding 96-well plates for enzyme-linked immunosorbent assays (ELISA) were from Costar (through Fisher Scientific, Leicestershire, UK). ELISA CytoSet™ kits were sourced from BioSource (Nivelles, Belgium). Bradford's reagent was used for the calculation of total protein concentration, bovine serum albumin (BSA) was used as the standard and sodium dodecyl sulfate (SDS) was used to solubilise the cell layer. Flu–Na and FITC-dex (4, 10, 20, 40 and 70 kDa) were used as fluorescent makers. Calu-3 cells were from the American Type Culture Collection (ATTC, Rockville, MD, USA) and were used between passages 36 and 54.

3. Apparatus

Light microscopy was performed with a Wilovert S inverted microscope (Hunt Wetzlar, Germany). Particle size measurements were performed with a Nikon Labophot light microscope (Tokyo, Japan), linked to an Acorn personal computer with particle size analysis software designed in-house. TER was measured using chopstick electrodes and an EVOM voltohmmeter (STX-2 and Evom G, World Precision Instruments, Stevenage, UK). Cell layers were disrupted using a Vibracell 400 cell sonicator (Sonics and Materials, Danbury, USA). Fluorescence was measured using a Cytoflour series 4000 fluorescent plate reader (Foster City, CA, USA). Ultraviolet (UV) absorption for ELISA readings was obtained using a Spectramax 190 (Molecular devices, Sunnyvale, USA). The vacuum pump and TSI were purchased from Copley Scientific (Nottingham, UK).

4. Methods

4.1. Adaptation of the TSI for particle delivery

A glass TSI was assembled as described in the British Pharmacopeia [16], apart from the absence of solution in the lower chamber (Fig. 1a). The adapter piece (B) was removed and parafilm wrapped around the base of the connecting tube to produce an attachment surface for the Transwell insert. The Transwell insert was then pushed onto the connecting tube until the tapered internal walls of the insert fastened firmly onto the parafilm (Fig. 1b). Thus, air flowing down the connecting tube was diverted through the lateral ports of the insert. This caused particles to exit the air stream through inertial impaction and deposit onto the cell layer. The system was developed initially using a cell-free Transwell support, with a glass coverslip placed in the insert to collect particles. Powder for deposition (~5 mg), which had been comminuted with a mortar and pestle, was placed in the centre channel of a custom-made glass dry powder insufflator (Fig. 2), which was sealed into place at the entrance of the TSI (Fig. 1a, position A). The 6-mm centre channel of the insufflator was occluded and the vacuum pump run at 60 L/min producing an airflow through the outer (air vent) channels. The powder was delivered by opening the centre channel of the insufflator, allowing the airflow to aerosolise the powder into the TSI. After a total of 5 s, the vacuum was turned off and the Transwell filter removed. The glass coverslip was removed from the insert, transferred to a microscope slide and 500 particles were selected at random and measured to quantify the geometric median mass diameter of each sample (μm) and the proportion <6.4 μm.

4.2. Particle deposition and compound transport across cell layers

Calu-3 cells were grown at an air interface and used between day 11 and 13 in culture as described previously [15]. The Transwell insert containing the cells was affixed to the TSI conducting tube in the lower chamber and the test powder was loaded into the dry powder insufflator and aerosolised as described above. After deposition of the particles, the Transwell insert was removed from the TSI and transferred to a well of a 24-well base plate

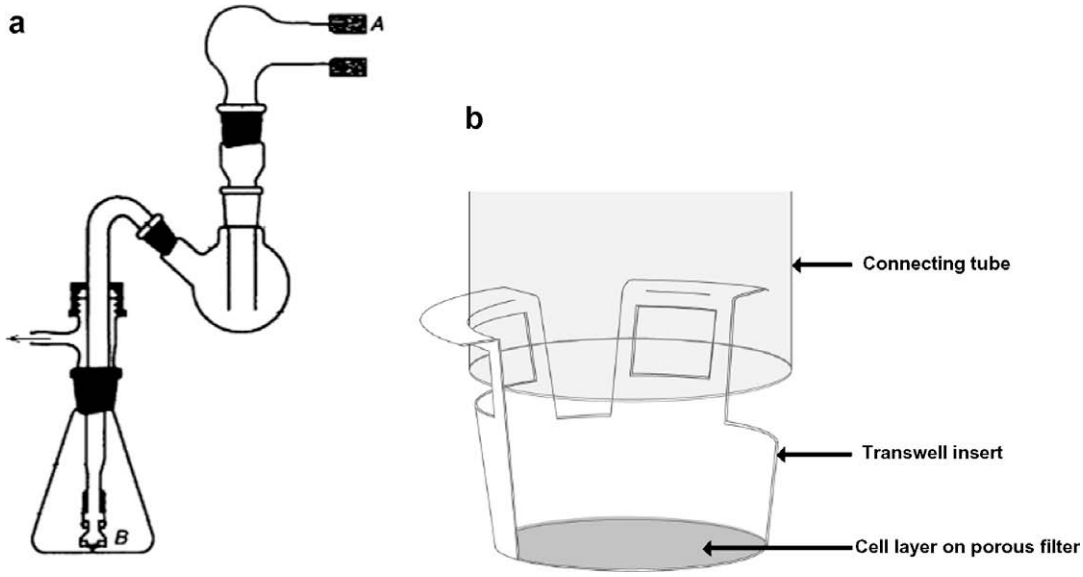

Fig. 1. (a) The twin-stage impinger (TSI) [with permission, 16]. (b) The cell layer-bearing Transwell is attached to the TSI at position B in (a). Particles suspended within the airflow travel vertically down the connecting tube and deposit via inertial impaction onto the cell layer, where the airflow is redirected laterally through the openings of the Transwell walls.

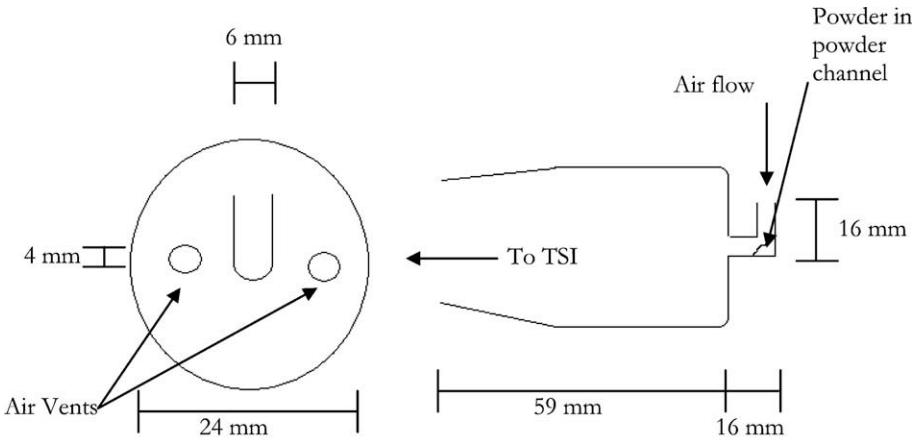

Fig. 2. Diagram of the bespoke dry powder insufflator device (not to scale). End on view of the two airflow ports and powder chamber in centre (left). Side-view of adapter (right). Powder can be seen in the insufflator powder channel. A seal is placed on the top of this tube when the pump is turned on, so that air only flows through the two circular side air vents. The seal is then removed and the air also flows through the powder channel and aerosolises the powder into the TSI via port A (Fig. 1a).

containing 1 ml of warmed HBSS (37 °C) and gently agitated to wash away any particles adhering to the outer surface. After 5 s it was removed, the outer-surface wiped dry, and transferred to a fresh well containing 600 μl of warm HBSS (receiver fluid). A sample (100 μl) of the receiver fluid was removed immediately and placed in a black 96-well plate to serve as a blank. At preset time points (up to 4 h), 100 μl samples of receiver fluid were removed and replaced with HBSS to maintain the well volume. At the final time point, the Transwell insert was removed from the well, the outer surface was wiped dry and the semi-permeable membrane and cell layer were cut from the plastic well using a scalpel and placed in 1 ml HBSS. The sample was homogenised using a cell sonicator at 40% of the full scale-setting for 30 s before a 100 μl aliquot was removed for the analysis. Where TER was measured after particle deposition or sham deposition (air only), 100 μl warmed HBSS was added to the apical side once the cell layer was removed from the TSI and placed in the 24-well base plate for TER measurement. Where particles were solubilised immediately after deposition (or where no particle deposition took place), a solution of the appropriate test compound (1 mg/ml) was added to the apical chamber after deposition, mixed gently and sampled to permit confirmation of the starting concentration. For all experiments cell layers were maintained at 37 °C on an orbital shaker rotating at 100 rpm.

Samples were analysed by fluorescence spectroscopy. Each sample in the 96-well plate was treated with a 1 mM NaOH solution (100 μl) then analysed using a fluorescent plate-reader using wavelengths of 480 nm excitation and 530 nm emission. The percentage of the mass transported was calculated from the cumulative mass transferred to the receiver chamber at each time point expressed as a ratio of the dose applied. Where particles were deposited and left to dissolve in the cell lining fluid, the initial dose was estimated from the sum of the mass having passed through the cell layer plus the mass recovered from the apical surface and in the cell layer at the final time point. Where P_{app} was calculated (Eq. (1)), the volume of the cell lining fluid assumed as 3.44 μl (see below).

4.3. Calculation of cell lining fluid volume

The volume of fluid on the surface of the cell layers was calculated using a dilution technique. Warmed flu–Na solution (10 μl, 0.01 μg/ml) was added into the cell layers, gently rotated and

repeatedly pipetted to mix the surface fluid present with the fluorescent solution for 1 min. After this, 5 μl was removed and assayed to measure the dilution.

4.4. IL-8. ELISA assay

FITC-dex 4 particles were deposited onto the cell layer and the Transwell was returned to the base plate containing cell culture medium and placed back into a cell incubator. After 24 h, 200 μl of cell culture medium was added to the apical chamber and mixed gently with the cell lining fluid. Samples (100 μl) of both the apical and basolateral compartments were then removed for the analysis of human IL-8 by ELISA according to the manufacturer's instructions. The control layer was not exposed to any treatment. To control for variations in total cell density, total protein was analysed using the Bradford assay [17].

4.5. Modelling of compound spreading

To calculate the extent of compound spreading from a point source into the plane of the cell lining fluid, Fick's second law of diffusion (Eq. (2)) was used as described in an earlier report [18].

4.6. Statistical testing

Statistical testing was performed by using SPSS version 11.0 software and data were analysed by one way ANOVA and Dunnett's post Hoc analysis, with significance reported if $P < 0.05$.

5. Results

5.1. Particle deposition to cell layers

Light microscopy of representative particles (FITC-dex 4 and FITC-dex 40) showed that >96% of the particles which were deposited in the Transwell were <6.4 μm in geometric diameter (data not shown). The microscopy confirmed that the TSI was effective in permitting only particles of a respirable size to travel to the lower chamber and that particles deposited discretely with an even distribution over the surface of a cell-free Transwell. TER was measured after deposition of particles onto Calu-3 cells to determine whether there was any detrimental effect upon the integrity of the model epithelial barrier. Experiments included cell layers that were:

(i) not exposed to air flow or particles and dextran solution was applied (control),
(ii) placed in the TSI and exposed to 5 s of air flow, followed immediately by the addition of dextran solution,
(iii) placed in TSI and exposed to 5 s of air flow with dextran particle deposition, followed immediately by the addition of dextran solution,
(iv) placed in the TSI and exposed to 5 s of air flow with dextran particle deposition, without any additional fluid added to the apical chamber.

In experiments (ii) and (iii) where the cells were placed in the TSI, a transient drop to 90% of the control TER value occurred, but this recovered to the original value within 10 min (data not shown). In experiment (iv), the cell layer remained air interfaced, preventing measurement of TER. The P_{app} of FITC-dex 4 applied as a solution (experiments ii and iii) confirmed that despite the 10% drop in TER, solute permeability was unaltered compared to control (P_{app} of $0.86 \pm 0.25 \times 10^{-6}$ cm/s and $0.67 \pm 0.11 \times 10^{-6}$ cm/s, respectively, compared to the control of $0.71 \pm 0.18 \times 10^{-6}$ cm/s; mean ± SEM, $n = 7–15$, $P \geqslant 0.05$). No change in IL-8 secretion in either apical or basolateral directions occurred after the deposition of FITC-dex 4 particles (iv; Fig. 3) compared to the control (air only (i), $P \geqslant 0.05$). These data show that no change in cell layer permeability occurred and no pro-inflammatory response was generated by the deposition procedure.

5.2. Solute transport in the cell layer

The transport rate of FITC-dex 4 across the Calu-3 layer in the absorptive direction over 4 h (Fig. 4) was unchanged compared to control (i) after exposure to airflow (ii) or particle deposition (iii) when FITC-dex 4 solutions were added to the apical chamber. An ~20-fold increase in FITC-dex 4 transport rate compared to application as a solution occurred following deposition as particles with no addition of fluid to the apical chamber (iv). Similar significant increases in transport rate were seen for the other FITC-dex molecules (10, 20, 40 and 70 kDa), ranging between a 9 and 21-fold increase after deposition as a particle compared to as a solution.

5.3. Compound distribution at cell surface

Rapid dissolution and diffusion was observed within the cell lining fluid to generate a homogeneous apical solution of FITC-dex within the first minute after particle deposition (by visual inspection). A simple theoretical model of spreading following dissolution at the site of deposition of flu–Na and FITC-dex 70 in the cell lining fluid was applied using Eq. (2) [19]. The decline in concentration as a function of the radius from the point of deposition at different times was calculated and plotted (Fig. 5). For both the largest and smallest molecules, diffusional spreading was shown to occur rapidly with the concentration excess at the point of impact declining rapidly between 2 and 10 s after deposition. These results provide theoretical support for the observation that the particles dissolved quickly and were homogeneously dispersed in the apical fluid.

5.4. Estimating P_{app} after aerosol deposition

The volume of fluid on the apical surface of the Calu-3 cell layers was estimated using the dilution technique to be 3.44 ± 1.90 μl (mean ± SEM, n = 16; samples being taken over 3 separate cell passages). Thus, P_{app} was calculated from the measured transport rate and known surface area for diffusion, with the initial concentration of compound in cell lining fluid after deposition derived from the mass deposited (calculated from the mass balance at $t = 240$ min), the 3.44 μl cell lining fluid, with the assumption that

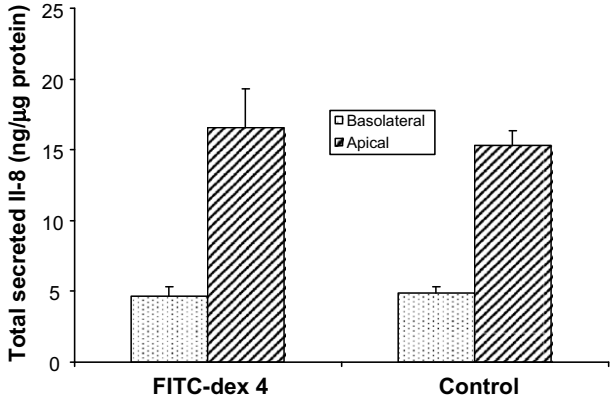

Fig. 3. Total IL-8 secretion by Calu-3 cell layers after 24 h following deposition of FITC-dex 4 particles using the TSI or control (no treatment). Data represent $n = 5$, mean ± SD.

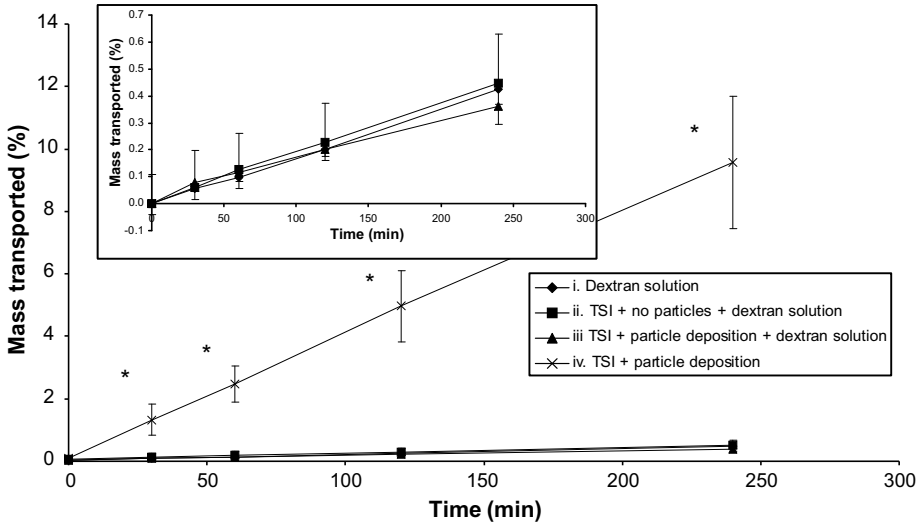

Fig. 4. Transport rate of FITC-dex 4 across Calu-3 cell layers after (i) application as a solution, (ii) exposure of cell layer to airflow in the TSI followed by the application of FITC-dex solution, (iii) exposure of cell layer to airflow and the deposition of FITC-dex 4 particles in the TSI, followed by the application of dextran solution or (iv), exposure of cell layer to airflow and deposition of FITC-dex 4 particles which were allowed to dissolve in cell lining fluid. The inset Figure is an enlarged scale between 0–0.8% mass transported of the main Figure. Data represent $n = 7–15$ (mean ± SEM on 3–4 separate occasions). *Statistically different to control (i) ($P < 0.05$).

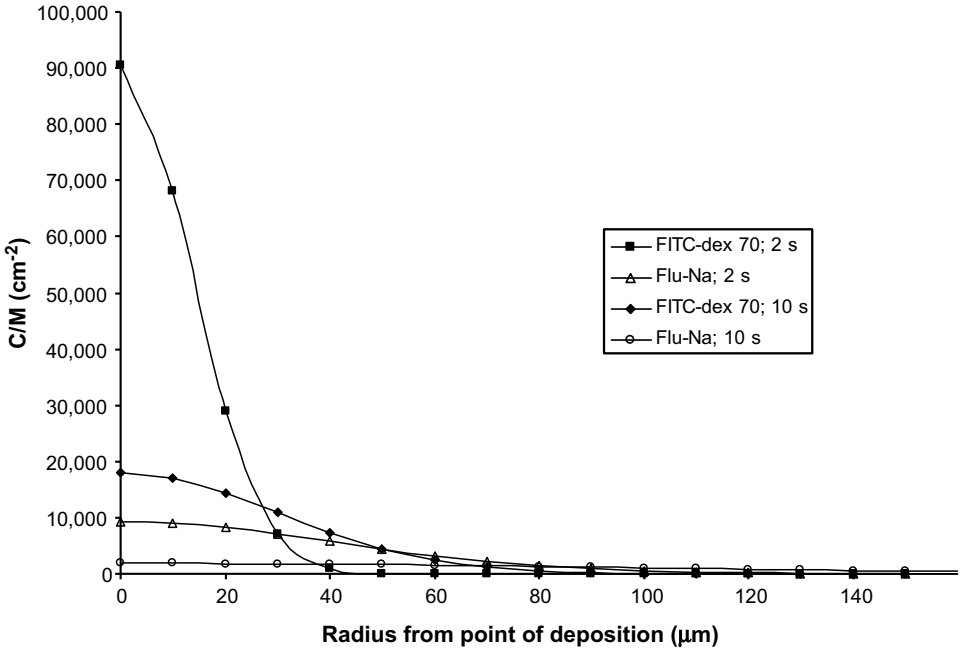

Fig. 5. The predicted lateral spreading profile of compounds through the cell lining fluid from a point source can be plotted at varying times (2 and 10 s) calculated from Eq. (2) using the diffusion coefficients in mucus (flu–Na; 4.29×10^{-6} cm^2 s^{-1} (molecular weight of 0.396 kDa) and FITC-dex 70; 0.44×10^{-6} cm^2 s^{-1}) [28]. C is the mass of compound per cm^2 and M is the mass of compound initially deposited at the central point.

homogeneity is quickly achieved by rapid particle dissolution and lateral diffusion of the solute. Sink conditions (defined as the receiver chamber concentration being <10% of donor chamber concentration) were maintained during all experiments. The permeability of the FITC-dex 4 after deposition as aerosolised particles was compared to measured P_{app} values obtained when the same FITC-dex was applied as a solution. Despite the 20-fold higher transport rate, the estimated P_{app} was unchanged ($P \geqslant 0.05$) when compared to the control (P_{app} following particle deposition was 1.39-fold ± 0.41 the value for the solution control; mean ± SEM, n = 10–15 with experiments conducted over 3 separate passages).

5.5. In vitro–in vivo correlation

After aerosolisation and deposition of the FITC-dex particles onto Calu-3 cell layers, the absorptive transport rates of the compounds across Calu-3 cells were correlated with estimated clearance rates of similar molecular weight dextrans from the canine lung [18]. Pulmonary clearance of the FITC–dex used in this study was estimated using the linear relationship between known log10 pulmonary clearance and log10 dextran molecular weight (3–500 kDa). A strong positive correlation ($r^2 = 0.918$) was found between the transport of aerosolised dextran in Calu-3 cell layers and *in vivo* clearance from the canine lung (Fig. 6).

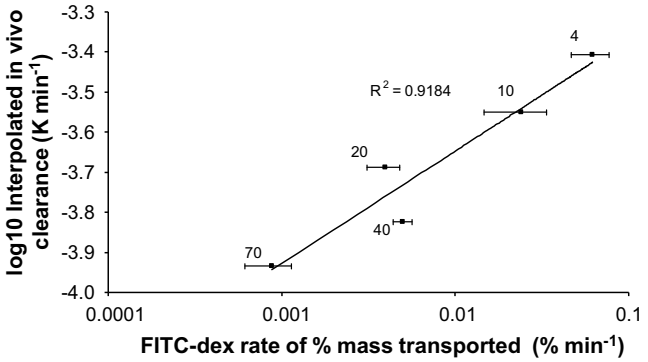

Fig. 6. Relationship between experimental dextran permeability in Calu-3 cells measured in this study and the interpolated clearance rates through the canine lung (derived from [18]). Calu-3 data, $n = 5 \pm$ SD. Dextran molecular weight (kDa) indicated adjacent to the data points.

6. Discussion

In this study, a system for application of respirable aerosols to layers of epithelial cells modelling the bronchial region of the lung is reported. This system caused no measurable adverse effects to the cell layer and allowed measurements of permeability of the deposited compound to be obtained. To date there have been few published attempts to replicate the aerosol deposition that occurs *in vivo* using *in vitro* models. Classically, in toxicological and transport studies, compounds of interest have been applied simplistically as pre-dissolved test compounds in solution. This precludes any consideration of the importance of aspects relating to particle-cell layer interaction that may occur *in vivo*.

Particle velocity in the reported system was comparable to that which occurs *in vivo*. In the system described, particles travelling within an airflow controlled at 60 L/min through a 0.33 cm^2 orifice (the bottom of the connecting tube) are moving with a velocity of 30 cm/s. *In vivo*, the velocity of particles is estimated to vary from 300 cm/s (in the trachea/main bronchial region) to 3 cm/s in the respiratory bronchioles (generations 15–16) after a sharp inspiration [20]. Dosimetry to the cell layers ranged between 1.5 and 150 μg/cm^2, dependant on the FITC-dex applied. In the context of therapeutic drug payloads, the bronchial regions may receive a bronchodilator dose of around 20 μg via an inhaler [21], equating to approximately 6 ng/cm^2, assuming equal distribution of the particles throughout the bronchial region. In reality, hotspots of deposition are present at the bifurcations of the airways, resulting in much higher concentrations than produced on the walls of the bronchial airways. Therefore in practice, it is challenging to work with a realistic *in vivo* dose using *in vitro* methods such as these. The cell lining fluid volume calculated within this study also exceeded the depth of the majority of the epithelial lining fluid found *in vivo*. A volume of 3.4 μl spread evenly over 0.33 cm^2 would produce a depth of ~100 μm, although a meniscus did form at the walls of the Transwell. This high value was partly due to the rehydration of the mucus layer upon TER measurement. *In vivo*, the mucus lining ranges from around 5 μm from the respiratory bronchioles to around 100 μm in the largest airways [22].

A marked difference in the transport rate was observed for hydrophilic compounds when deposited as an aerosol compared to their application as a solution. However, the P_{app} after particulate administration was equivalent to that when applied as solution, indicating that the increased rate of compound transfer following aerosol administration *in vitro* was explicable by the high driving concentration (generated by dissolution in the low volume of apical fluid), rather than any change in the local permeability of the cell layer itself. This scenario is applicable for inert hydrophilic molecules that dissolve and spread rapidly in cell lining fluid. Compounds may have other effects on the cell layer permeability when delivered in their environmental form. For example, Qi and co-workers [23] deposited heparin particles on Calu-3 cell layers, allowing them to dissolve on the cell surface [23]. This resulted in a detrimental effect on TER and an increased rate of paracellular transport compared to the same quantity of heparin applied in solution. It was proposed that the focal high concentrations of heparin produced at the points of particle deposition induced disruption to Zona occludens 1 (ZO-1) localisation in the tight junction and associated actin cytoskeleton. In addition, differential effects of plant volatiles have been observed after application to layers of bronchial epithelial cells as a gas or dissolved in a liquid [24].

A limitation of using the TSI as a device to deliver particles is that only one cell layer at a time can be dosed, leading to variability in deposition levels and making it labour-intensive with an extended dosing time per cohort of cells. The MSLI and ACI which Fiegel et al. [12] and Cooney et al. [13] employed, respectively, are more convenient as it is possible to dose multiple cell layers at once. However repeat dosing for longer term toxicity studies would be difficult due to the lack of sterility of all these particulate administration systems. Nevertheless, such systems achieve the objective of applying aerosols onto lung epithelial cell layers *in vitro*. They act as a 'platform technique' in which many types of aerosols could be applied to respiratory cell cultures that model different regions of the respiratory tract. Cell layers modelling the nasal epithelium can be placed in the upper chamber of the TSI [14] and a bronchial epithelial model placed in the lower. The MSLI and ACI also offer the potential of placing alveolar cell types in/on the lower chambers/plates to permit deposition of aerosols <2 μm.

In conclusion, dextrans of different MW were applied as powder aerosols to the Calu-3 cell layers and the resulting transepithelial transport rates monitored. When compared to clearance rates of similar molecular weight dextran compounds from the canine lung, a strong correlation was obtained. The permeability of a variety of compounds in respiratory cell culture models has been correlated with absorptive clearance in *in vivo* and *ex vivo* models previously [13,25–27]. However, none of these studies administered compounds to cell layers via aerosolisation and allowed the particles to dissolve in cell surface fluid. For lipophilic compounds, or aerosols with larger particle diameters, dissolution in epithelial surface fluid would be expected to play an important role in determining respiratory absorption rates. In this situation, the *in vitro* delivery system and experimental protocols reported in this article become highly relevant and may prove to be more realistic than conventional methods for predicting systemic exposure *in vivo*, since particle dissolution rate is incorporated as an experimental factor.

Acknowledgments

The authors are grateful to Unilever plc for the funding of this work and to David Lockley for his helpful guidance. The authors are also grateful for the help of Grace Grainger in the drawing of the Transwell insert.

Appendix A. Apparent permeability (P_{app})

$$P_{app}(\mathrm{cm/s}) = \frac{\text{Rate } (\mu g/s)}{\text{Transwell surface area}(cm^2) \times \text{ Starting concentration}(\mu g/cm^3)} \quad (1)$$

where

Rate = rate of change in cumulative mass transported.

Starting concentration = initial concentration in the donor chamber

Appendix B. Spreading of a solute from a point source into a plane

$$\frac{C}{M} = \frac{e^{-(r^2/4Dt)}}{4\pi Dt} \quad (2)$$

where

C = quantity of solute per area (mg/cm^2)
M = quantity deposited at the central point (mg)
D = diffusion coefficient in mucus (cm^2/s) [28]
t = time (s)
r = radius (μm)
π = pi

References

[1] G. Borchard, M.L. Cassara, P.E.H. Roemele, B.I. Florea, H.E. Junginger, Transport and local metabolism of budesonide and fluticasone propionate in a human bronchial epithelial cell line (Calu-3), J. Pharm. Sci. 91 (2002) 1561–1567.

[2] C. Westmoreland, T. Walker, J. Matthews, J. Murdock, Preliminary investigations into the use of a human bronchial cell line (16HBE14o-) to screen for respiratory toxins *in vitro*, Toxicol. in Vitro 13 (1999) 761–764.

[3] C. Riganti, E. Aldieri, L. Bergandi, M. Tomatis, L. Fenoglio, C. Costamagna, B. Fubini, A. Bosia, D. Ghigo, Long and short fiber amosite asbestos alters at a different extent the redox metabolism in human lung epithelial cells, Toxicol. Appl. Pharmacol. 193 (2003) 106–115.

[4] S. Rappeneau, A. Baeza-Squiban, F. Marano, J.H. Calvet, Efficient protection of human bronchial epithelial cells against sulfur and nitrogen mustard cytotoxicity using drug combinations, Toxicol. Sci. 58 (2000) 153–160.

[5] M.E. Cavet, M. West, N.L. Simmons, Transepithelial transport of the fluoroquinolone ciprofloxacin by human airway epithelial Calu-3 cells, Antimicrob. Agents Chemother. 41 (1997) 2693–2698.

[6] J.P. Evans, N. Tudball, P.A. Dickinson, S.J. Farr, I.W. Kellaway, Transport of a series of D-phenylalanine-glycine hexapeptides across rat alveolar epithelia *in vitro*, J. Drug Target. 6 (1998) 251–259.

[7] I. Pezron, R. Mitra, D. Pal, A.K. Mitra, Insulin aggregation and asymmetric transport across human bronchial epithelial cell monolayers (Calu-3), J. Pharm. Sci. 91 (2002) 1135–1146.

[8] S. Boland, A. Baeza-Squiban, T. Fournier, O. Houcine, M.C. Gendron, M. Chevrier, G. Jouvenot, A. Coste, M. Aubier, F. Marano, Diesel exhaust particles are taken up by human airway epithelial cells *in vitro* and alter cytokine production, Am. J. Physiol. Lung Cell. Mol. Physiol. 276 (1999) L604–L613.

[9] M. Bur, H. Huwer, C.M. Lehr, N. Hagen, M. Guldbrandt, K.J. Kim, C. Ehrhardt, Assessment of transport rates of proteins and peptides across primary human alveolar epithelial cell monolayers, Eur. J. Pharm. Sci. 28 (2006) 196–203.

[10] M. Aufderheide, J.W. Knebel, D. Ritter, A method for the *in vitro* exposure of human cells to environmental and complex gaseous mixtures: application to various types of atmosphere, ATLA—Alt. Lab. An. 30 (2002) 433–441.

[11] J.W. Knebel, D. Ritter, M. Aufderheide, Development of an *in vitro* system for studying effects of native and photochemically transformed gaseous compounds using an air/liquid culture technique, Toxicol. Lett. 96-7 (1998) 1–11.

[12] J. Fiegel, C. Ehrhardt, U.F. Schaefer, C.M. Lehr, J. Hanes, Large porous particle impingement on lung epithelial cell monolayers – toward improved particle characterization in the lung, Pharm. Res. 20 (2003) 788–796.

[13] D. Cooney, M. Kazantseva, A.J. Hickey, Development of a size-dependent aerosol deposition model utilising human airway epithelial cells for evaluating aerosol drug delivery, ATLA – Alt. Lab. An. 32 (2004) 581–590.

[14] B. Forbes, S. Lim, G.P. Martin, M.B. Brown, An *in vitro* technique for evaluating inhaled nasal delivery systems, STP Pharm. Sci. 12 (2002) 75–79.

[15] C.I. Grainger, L.L. Greenwell, D.J. Lockley, G.P. Martin, B. Forbes, Characterisation of an epithelial cell line for a permeability model of the lung, Pharm. Res. 23 (2005) 1482–1490.

[16] British Pharmacopoeia. Appendix XII F. Aerodynamic assessment of fine particles – fine particle dose and particle size distribution, Figure 12F-1. 1 (2004) 254–255.

[17] M.M. Bradford, A rapid and sensitive method for the quantitation of microgram quantities of protein utilizing the principle of protein–dye binding, Anal. Biochem. 72 (1976) 248–254.

[18] R.M. Effros, G.R. Mason, Measurements of pulmonary epithelial permeability *in vivo*, Am. Rev. Respir. Dis. 127 (1983) S59–S65.

[19] J. Crank, The Mathematics of Diffusion, Oxford University Press, London, 1975.

[20] E.R. Weibel, in: E.R. Weibel (Ed.), Morphometry of the Human Lung, Springer-Verlag, London, 1963.

[21] H. Bisgaard, B. Klug, B.S. Sumby, P.K. Burnell, Fine particle mass from the Diskus inhaler and Turbuhaler inhaler in children with asthma, Eur. Respir. J. 11 (1998) 1111–1115.

[22] J.H. Widdicombe, J.G. Widdicombe, Regulation of human airway surface liquid, Respir. Physiol. 99 (1995) 3–12.

[23] Y.W. Qi, G.L. Zhao, D.F. Liu, Z. Shriver, M. Sundaram, S. Sengupta, G. Venkataraman, R. Langer, R. Sasisekharan, Delivery of therapeutic levels of heparin and low-molecular-weight heparin through a pulmonary route, Proc. Natl. Acad. Sci. USA 101 (2004) 9867–9872.

[24] P. Bonsi, F. Zucco, A. Stammati, Two *in vitro* models for gas-phase exposure to volatile compounds, ATLA – Alt. Lab. An. 30 (2002) 241–247.

[25] F. Manford, A. Tronde, A.B. Jeppsson, N. Patel, F. Johansson, B. Forbes, Drug permeability in 16HBE14o- airway cell layers correlates with absorption from the isolated perfused rat lung, Eur. J. Pharm. Sci. 26 (2005) 414–420.

[26] N.R. Mathias, J. Timoszyk, P.I. Stetsko, J.R. Megill, R.L. Smith, D.A. Wall, Permeability characteristics of Calu-3 human bronchial epithelial cells: *in vitro–in vivo* correlation to predict lung absorption in rats, J. Drug Target. 10 (2002) 31–40.

[27] A. Tronde, B. Norden, A.B. Jeppsson, P. Brunmark, E. Nilsson, H. Lennernas, U.H. Bengtsson, Drug absorption from the isolated perfused rat lung – correlations with drug physicochemical properties and epithelial permeability, J. Drug Target. 11 (2003) 61–74.

[28] B.T. Henry, J. Adler, S. Hibberd, M.S. Cheema, S.S. Davis, T.G. Rogers, Epi-fluorescence microscopy and image analysis used to measure diffusion coefficients in gel systems, J. Pharm. Pharmacol. 44 (1992) 543–549.